Dynamic Pre-Grasp Planning when Tracing a Moving Object Through a Multi-Agent Perspective

Michael Bowman, and Xiaoli Zhang*, *Member, IEEE*

***Abstract*—While a human is tracking a moving object to prepare for later grasping, we naturally change our hand pose to generate optimal pre-grasp to avoid post-grasp adjustment. Robot hand controllers need dynamic pre-grasp planning capability, so they are not limited in dynamic tracking and catching tasks. To fill this gap, we explore the feasibility of using a two-stage optimization method to enable dynamic pre-grasp planning of individual fingers while tracking a moving object to ensure a later successful grasp. The first stage adopts multi-agent pursuit to partition the search space on the object surface. The method allows each finger to consider its immediate surroundings in a local view instead of globally determining the best location for all fingers. The search space for each finger is dramatically reduced since sensible alternatives are the ones left after pruning. Each finger goal location acts independently yet coordinates with others to achieve the goal of covering the object. In the second stage, four different goal point movement strategies are presented to impact the finger goal location in their respective search space to demonstrate the ability to facilitate different needs of the task and requirements of the designer. Dynamic finger goal adaption is obtained by iteratively updating these two stages. The approach is consistent in different scenarios for the object.**

I. Introduction

People naturally track falling objects and adjust their hand posture in anticipation. This is seen in common tasks such as tossing car keys to a friend or playing catch with a kid. Often when teaching a kid to catch, we instruct them to keep their hands up and predict where the ball will land. This phenomenon is known as pre-shaping [1]. Pre-shaping depends upon time and prior hand configurations as the human anticipates how the object will conform to their hand. An example of this is juggling as shown in Figure 1a. Two different postures are shown in Figure 1b. The first is with inappropriate pre-shaping which results in a recovery to a more proper pose of the hand (top of Figure 1c). Further, the type of "catch" is important as it minimizes the recovery motion and allows for faster manipulation post catch (bottom of Figure 1c). The ramifications of an inappropriate pre-grasp pose lead to either 1) a suboptimal grasp configuration occurs, and an unstable grasp of the object results in a failure, or 2) too much energy is consumed and distance to travel to correct to an appropriate pose. Therefore, generating a pre-shaping posture is critical for determining the overall success for grasping a moving object.

Michael Bowman is a PhD Candidate in the Department of Mechanical Engineering at Colorado School of Mines, Golden, CO 80401 USA (email: mibowman@mines.edu).

*Xiaoli Zhang is an Associate Professor in the Department of Mechanical Engineering at Colorado School of Mines, Golden, CO 80401 USA (*corresponding author, phone: 303-384-2343; fax: 303-273-3602; email: xlzhang@mines.edu).

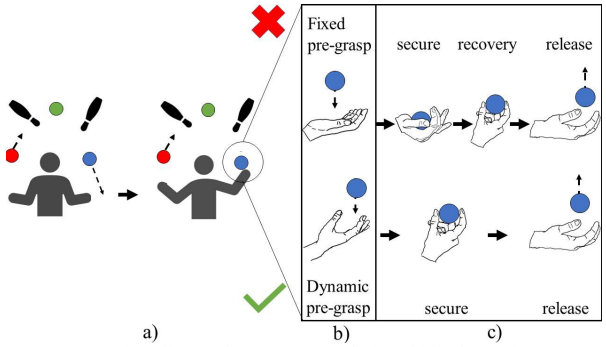

Figure 1: a) a juggling task as an example in which dynamic pre-grasp planning is essential for task success. b) shows two potential strategies for catching the object. The top row is a fixed pre-grasp pose. The bottom is a dynamic pre-grasp pose. c) is the consequences of choosing b). The fixed pre-grasp pose requires post grasp recovery before releasing. The dynamic pre-grasp pose minimizes post-grasp adjustment if any. This work focuses on developing a dynamic pre-grasp planning method to help robotic structures to grasp moving objects.

The potential avenues to achieve the above tasks include tracking and tracing an object commonly found in hitting tasks [2], and predefined static poses before a grasp [3][4][5]. Yet, neither of these solutions are quite suitable achieve the task. Although the tracking approaches can dynamically adjust to a moving object, the hand is simplified by not considering multi-finger grasping dynamics. It is necessary to apply this dynamic adjustment to individual fingers to achieve a better grasp solution—a finger dominated grasp (precision grasp) allows for rotations or adjustments of the object, while a palm dominated grasp (power grasp) allows for greater grasp stability. Synergy-based approaches create an interdependent model and can replicate these different grasp styles; however, they lack the ability to generate independent finger motion [6][7]. Specifying every predefined pre-grasp pose on moving objects can become tedious and tricky as the uncertainties can cause instability, and undesired results. By considering each time point as static, the pre-grasp pose trajectory is susceptible to dynamic disturbances and uncertainties in the environment. Therefore, pose generation must be able to recover from uncertainties in the environment and from ill-positioned initial conditions. Ideally dynamic pre-grasp planning needs a fast, parallel process (multi-agent finger control) to handle dynamic environmental changes, disturbances, and task constraints.

The goal of this work is to create a dynamic pre-shape pose planning method to help control robotic structures to grasp a moving object. A technique in multi-agent pursuit paired with grasping dynamics is employed to 1) reduce the available search space for a given task, 2) simplify the complexity of robotic structures and controllable parameters which are

difficult to determine in real time, and 3) improve fast kinematic solutions which are cumbersome to develop for generalized systems. This paper does not focus on robotic structure design, nor inverse kinematic solutions. The contributions of this work are three-fold:

1) Developed a dynamic convex partitioning for each projected contact point (projected finger goal point) on an object (called safe regions). Inspired by a multi-agent perspective—we treat each finger through a local viewpoint with safe regions—the search space for potential poses are dramatically reduced since sensible alternatives are the ones left after pruning. Further, the safe regions are independently found where each finger does not need to be aware of all the global environments, just its nearest surroundings, which avoid undesired surfaces of an object. The safe regions can also depend upon physical capabilities of robotic hands/fingers.
2) Determining the placement and movement of the projected contact points (centroid) within a safe region through pose estimation of the object. The pose estimation allows for dynamic adaptation of the centroids by providing lookback and lookahead capabilities. Within each safe region, finding the right contact point is critical. We present four separate strategies (one based on position tracking and three are based on optimizing grasp matrix measures) to determine the placement given the potential candidates. This paper demonstrates how to find the centroid of safe regions (fingers) independently and how to apply coupling between centroids (e.g. fingertips, finger joints).
3) Validate and demonstrate robustness (through grasp quality metrics) of determining the contact points on a moving object through different object property scenarios such as speed, size, number of contact points needed.

II. Related work

In robotic grasping, a recent resurgence of effort has been put in to reduce the needed input dimensions by exploring and expounding the concept of synergies [6][8][9]. Synergies attempts to mimic human-like interdependence muscle-tendon motion. This is further extended to be used in underactuated robotics [10]. Other work in grasping has presented approaches in understanding the interdependence relationship of a human hand's degrees of freedom [11]. However, the dexterity of robotic hands can surpass that of the human hands due to independent control of each joint. Independence of each joint should be used to our advantage as they this allows each finger to determine their own goal location locally. However, to our knowledge treating each finger and palm as multi-agents has been rarely reported. The platforms which exist for controlling models only focus on the kinematic hand postures globally [12][13]. Since these approaches rely on synergies (interdependent finger model), the possible finger goals may not cover all possible poses or could lead to erratic motion of the hand. Further, these planners focus on objects with static positions. Decentralizing the mechanisms for goal locations by each finger to a local viewpoint will allow for a reduction in total search space, faster response time, and simplify the kinematic solvers by relieving them of the burden to find finger goal locations.

Interacting with moving objects is often simplified to striking tasks such as robot arms [14], or quadcopters [15] playing ping pong. The motions generated demonstrate that it is possible to achieve a good approach positions through tracking a moving object on board [16]. Even in the event of poor starting conditions [2]. Other similar trajectory planners have quadcopters catch a ball [17][18]. However, they do not consider grasping dynamics. In [18], they use multiple quadrotors tied to a net to catch and throw a ball, however, this is a simplification of the grasping task as they are not considering grasp dynamics. In [19], pose estimation of objects is considered for a controller that switches between a local and global planner. However, as in [20], the grasp models are learned by humans rather than analytical. Without considering the dynamics in the modeling process, this leaves little opportunity for these techniques to be extended to other object interaction scenarios.

When most platforms attempt to determine where and how to grasp objects, they attempt to optimize form closure or at the least force closure [21]. A common approach to form closure is referred to as caging [3][22]. Force closure is the relaxed case of form closure where friction forces help balance the object wrench [3]. These grasp measures often are viewed as static; they do not consider the temporal aspects of the contact points as they move. This too is reflected when attempting to collect human hand motion to create contact maps. The contact maps, developed through heat signatures [23] and motion tracking [24], of human hand motions provide good insights into how people contact various static objects. However, we view the moving object scenario as more challenging (as seen in Figure 1a) due to a less forgiving environment. A necessary study needs to be conducted into the efficacy of these metrics for dynamic objects. The repercussions of task failure are much higher leaving little to no chance for recovery and replanning of a poor grasp pose.

III. Methods

A. Developing Safe Regions by Each Finger

To ensure each finger's contact point does not overlap, act independently, and provide reasonable reachability an approach used in multi-agent pursuit tasks called Obstacle-Aware Voronoi Cells (OAVC) [25] can be employed to ensure the appropriate coverage of objects. Further, this approach can be used to follow the center of mass of an object through pose estimation [25] which will be explained in the next subsection. The goal of the OAVC is to find a safe region, S_i, for a projected finger contact point, $c_i \in R^3$, of a workspace, $Y \in R^3$, consisting of obstacles of $Z \in R^3$. For consistency, q denotes points in Y, while z_j denotes obstacle points j in Z. Y is determined based on shape related features such as object convexity and object related features such as material. The OAVC algorithm is given by Equation (1):

$$S_i = \{q \in Y \mid \|c_i - q\|^2 \leq \left\|z_j - q\right\|^2 - w_{ij}, j \in Z \; and \; \|c_i - q\|^2 - h_i \leq \|c_k - q\|^2 - h_k, k \in \{1, \dots, n\} \neq i\} \quad (1)$$

where h_i is a weighting term to describe the physical capabilities (such as maximum providable force or the degree

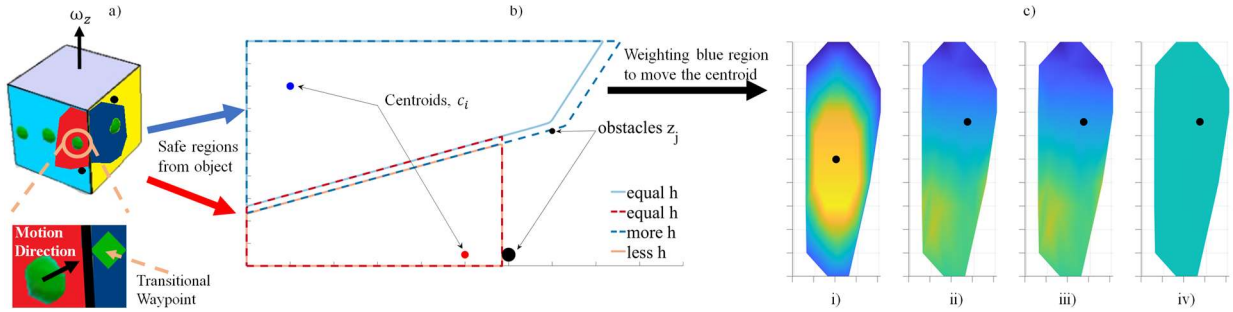

Figure 2: a) Demonstrates safe regions(blue and red zones) on an cube with 2 placed obstacles (locations we do not want the fingertips to touch). b) 2-D representation of different safe regions(dashed vs solid) depending on the weighting of h_i. The z_j represents obstacles. The smaller regions occur due to the smaller weighting value of h_i while larger weighting values lead to larger regions. This corresponds to making to the capabilities larger or smaller. In the case study of this paper h_i is weighted and considered through the fingertip dimensions. c) The weighting heatmaps for a single contact point. The black dot on each subplot corresponds to the new centroid location according to the respective weighting schemes. i) represents the position tracking, ii) represents b_n^{MSV}, iii) represents b_n^{GII}, iv) represents b_n^{VEW}. The b_n^{GII} method is directly proportional to the b_n^{MSV} which is the reason the heat maps are incredibly similar.

of importance of a single agent i.e., thumbs are more useful than little fingers) and attributes of the projected finger contact point c_i [26]. In the context of this paper, the size of the finger contact points was considered. The w_{ij} is defined in equation (2):

$$w_{ij} = 2\,R_j\|c_i - z_j\| - \|c_i - z_j\|^2 \quad (2)$$

where R_j is the radius of obstacle z_j [27]. Although these equations have been geared towards cartesian points for this paper, the algorithm is able to handle higher dimensions including forces, torques, or other physical capabilities of the finger joints. Obstacles can be user defined where certain regions on an object must be ignored due to task constraints (Figure 1a, grasp the top of the bowling pin, not the bottom) or hazardous reasons (robot harms itself or the environment). Figure 2b illustrates a 2-D representation of the Voronoi cell with obstacles. Capability changes of h_i can impact location of the boundaries (blue lines change). By finding each S_i, the search space for contact point selection can be reduced, where the next section discusses determining which is the most suitable location for the projected finger contact point c_i.

B. Determining Contact Points

1) Position Tracking Centroid Strategy

Determining the centroid of the safe region decides the next c_i within a S_i. Each c_i follows a parallel procedure where they independently determine their subsequent motion based off of the motion of the object. A Kalman filter is used for pose estimation of the object's center of mass. The Kalman filter collects measurement data (through image processing techniques [28][29] or in simulated environments [30]) and refines the estimation of the object pose. The Kalman filter creates a mean, μ, and a covariance matrix, Σ, to inform the S_i of the potential distribution of the pose. A Gaussian estimation has been used in multi-agent systems to estimate the location of the points [31] and is shown in equation (3). q_n is the points within a S_i, and b_n corresponds to the probability density of the point. The probability density is then used as a weighting scheme to determine the best location to move the centroid as shown in equation (4). d is the vector length of q_n.

$$b_n = P(q_n, \mu, \Sigma) = \frac{1}{\sqrt{|\Sigma|(2\pi)^d}} e^{-\frac{1}{2}(q_n-\mu)\Sigma^{-1}(q_n-\mu)^T} \quad (3)$$

$$c_i = \frac{\sum_{n=1}^{N} b_n q_n}{\sum_{n=1}^{N} b_n} \quad (4)$$

The resulting c_i is the centroid for the next iteration where the process does another iteration of determining S_i and c_i. With each iteration updating c_i, motion constraints can be imposed to ensure no combination of contact points lead to an infeasible grasp.

2) Alternative Centroid Determination Strategies

The weighting of q_n within S_i can be determined in other methods which include grasp measures involving the grasp matrices [3]. Three common measures are employed: the minimum singular value, grasp isotropy index, and volume of ellipsoid. Equation (5) is the minimum singular value (Q_{MSV}) of the grasp matrix (G) where it determines how near the grasp is to a singularity. Generally, the larger the value indicates a better grasp. Note, G_{q_n}, refers to the partial grasp matrix at point q_n.

$$b_n^{MSV} = \sigma_{min}\left(G_{q_n}\right) \quad (5)$$

Equation (6) is the grasp isotropy index (Q_{GII}), where the goal is to look at the uniform contribution of the contact points. The metric seeks to have equal contributions across all contact points which the optimal grasp value is 1.

$$b_n^{GII} = \frac{\sigma_{min}\left(G_{q_n}\right)}{\sigma_{max}\left(G_{q_n}\right)} \quad (6)$$

Equation (7) is the volume of the ellipsoid (Q_{VEW}), where k is an arbitrary constant. The goal is to view the global contribution of all the contact points. Each singular value is weighted the same, however, cannot distinguish which contact points are contributing more than others to grasp. By maximizing the measure, the closer the grasp achieves an optimum grasp configuration.

$$b_n^{VEW} = k\sqrt{\left|G_{q_n}\,G_{q_n}^T\right|} \quad (7)$$

Determining c_i is used in the same fashion as equation (4). Figure 2c shows a comparison of weighted heat maps to describe the different centroid selection criteria for a single S_i, as well as the resulting centroid location for each criterion. The different centroid locations change depending on the probability density. The c_i^{MSV} and c_i^{GII} are nearly identical as they both rely on the Q_{MSV}, unlike the c_i^{VEW}. The updating process among pose estimation, the safe regions, and centroid determination is shown in Figure 3. This updating continues until a grasp occurs. The pose estimation provides updates for the object pose and twist, while also providing updates of sets Y and Z. The updated local S_i are then provided to

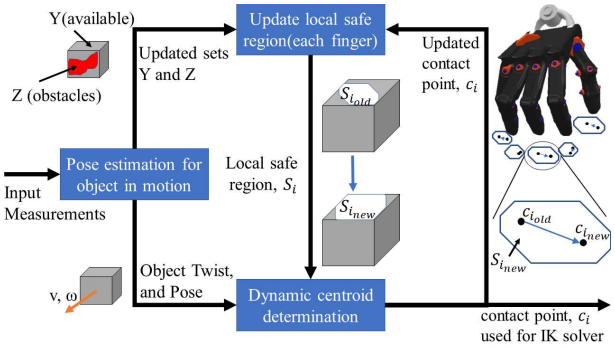

Figure 3: The overall system flow of dynamic contact goal points. The pose estimation of the object provides update sets Y and Z for the safe regions and object pose and twist for the centroid determination. The new centroids are set as the contact points which then provide a new point to update the safe regions.

determining the new c_i. These new c_i are then provided to back to update S_i and restart the process again.

3) Additional Evaluation Classifications

Each potential grasp is classified as indeterminate and graspable using null spaces (N) from equations (8) and (9) [3]. Equation (8) describes an indeterminate system by looking at the object twist in relation to the contact points. Any grasp with three or more non-collinear hard contacts will produce trivial solutions ($N(\boldsymbol{G^T}) = \mathbf{0}$). Equation (9) determines if the object is graspable—nontrivial solutions describe the tightness of a grasp and the wrench intensities necessary.

$$N(\boldsymbol{G^T}) \neq \mathbf{0} \quad (8)$$

$$N(\mathbf{G}) \neq \mathbf{0} \quad (9)$$

IV. Experiments and Results

A. Simulation Setup

For the experiments, simulations in the V-REP robotic simulation platform [30] were conducted since it is easier to show the S_i, c_i, and their updates (see supplementary video). To simulate the dynamic behavior of adapting c_i, a cube moving on a table was used. The cube has both translational and rotational movement. The c_i are made aware of physical constraints such as no occupation on the face of the cube in contact with the table. This constraint is implemented through the set Z discussed in the methods section. To further demonstrate adding constraints on the object surface, the top face was excluded from allowing c_i. The cube's center of mass was estimated by a Kalman filter. Five separate cases are conducted. The first two cases are object-based attributes of speed and size (cases b-e). The next two cases demonstrate the effective robustness through simulating damage to two fingers (going from 5 fingers to 3 fingers), and an example of a poor starting configuration for c_i (cases f-g). The last case compares the different centroid strategies (cases h-j). The summary of the conditions is summarized in Table I except for the centroid strategies which follow the base conditions. Three grasp measures—Q_{MSV}, Q_{GII}, and Q_{VEW}—are used to evaluate the grasp quality (object-based metrics) based on centroid locations. For each trial, every grasp was shown to be graspable through equations (8) and (9), thus the results are not shown for the sake of brevity.

TABLE I. Summary of Experimental Conditions

	Cases	Object Speed	Object Size	# of Points
Base	a)	v=0.001m/s, ω=0.0174rad/s	s=0.1m	5
Object Speed	b)	v=0.001m/s, ω=0.0087rad/s	s=0.1m	5
	c)	v=0.001m/s, ω=0.0349rad/s	s=0.1m	5
Object Size	d)	v=0.001m/s, ω=0.0174rad/s	s=0.07m h=0.075m	5
	e)	v=0.001m/s, ω=0.0174rad/s	s=0.2m h=0.1m	5
Damage	f)	v=0.001m/s, ω=0.0174rad/s	s=0.1m	5→3
Poor Start	g)	v=0.001m/s, ω=0.0174rad/s	s=0.1m	5

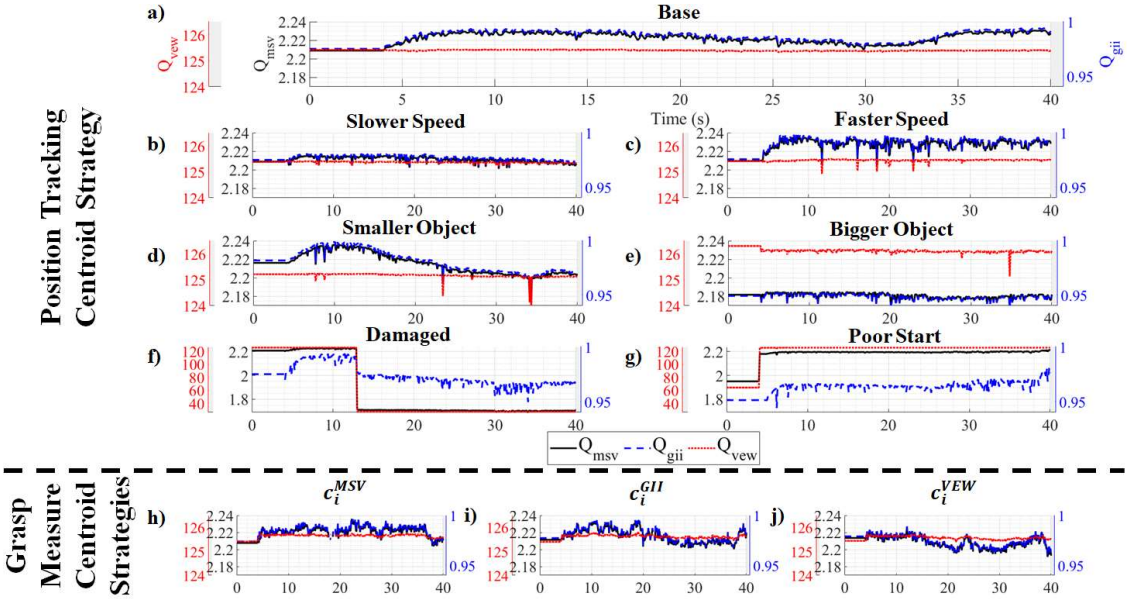

Figure 4: First 4 seconds are the static configuration. a) the base case, b) the slower object, c) the faster object, d) the smaller object, e) the bigger object, f) damage recovery from 5 to 3 contact points, g) poor start, h) c_i^{MSV} centroid, i) c_i^{GII} centroid , j) c_i^{VEW} centroid. The black line is the Q_{MSV} metric, the blue is the Q_{GII} metric, and the red is Q_{VEW} metric.

TABLE II. GRASP METRICS SUMMARY FOR POSITION TRACKING

	Fig. 4 Cases		Grasp Q_{MSV}	Grasp Q_{GII}	Grasp Q_{VEW}
Base	**a)**		**2.2307**	**0.9941**	**125.4403**
Object Speed	b)		2.2152	0.9804	125.4160
	c)		2.2357	0.9981	125.4970
Object Size	d)		2.2356	0.9989	125.2405
	e)		2.1846	0.9514	126.2973
Damage	f)	Static	1.6913	0.9494	26.8783
		Dyn.	1.7129	0.9770	27.0855
Poor Start	g)	Init	1.9508	0.9512	64.0511
		Dyn.	2.2159	0.9812	125.3789

a), b), c) f) have static grasp values of Q_{MSV} = 2.2089, Q_{GII} =0.9749, Q_{VEW} = 125.4176. d)'s static grasps values are of Q_{MSV} =2.2161, Q_{GII} =0.9818, Q_{VEW} =125.2092. e)'s static grasps values are of Q_{MSV} =2.1817, Q_{GII} =0.9489, Q_{VEW} =126.2972. f) shows after damage values. Static = static pre-pose; Dyn. = dynamic pre-pose.

B. *Position Tracking for Object Properties Results*

The simulation results are shown in Figure 4. The drops are a result of the discretization of Y; however, these are not significant as the scale on all three metrics show. Table II shows the maximum of the simulations' grasp qualities for a)-g) in Figure 4. Surprisingly, no significant difference is found, except for the damaged and ill starting condition cases. Trends still exist, for instance, the faster case has a higher Q_{GII} (0.9981) than the slower case (0.9804). This is likely due to the Kalman filter anticipating insignificant motion in the slower case thus the contact points are not as active resulting in lower uniformity. With object size we see a slight expected uptick in Q_{VEW} (126.2973) for the larger object compared to the smaller one (125.2405). The Q_{GII} for the larger object is lower (0.9514) than the smaller object (0.9989); likely due to the larger Y space which contact points can occupy so it is less likely the metric will have uniformity of contact points. The adaption solution remedied the damage case from the static values (Q_{MSV}=1.6913, Q_{GII}=0.9494, Q_{VEW}=26.8783) to (Q_{MSV}=1.7129, Q_{GII}=0.9770, Q_{VEW}=27.0855). The discrepancy of the quality of grasp between the base and the remedied solution is expected since higher values should occur with more contact points (Q_{MSV}=2.2307, Q_{GII}=0.9941, Q_{VEW}=125.24403) compared to the fewer contact points. Condition g) shows the ability to rebound to perform as well as other cases (Q_{MSV}=2.2159, Q_{GII}=0.9812, Q_{VEW}=125.3789).

TABLE III. CENTROID STRATEGIES GRASP METRICS SUMMARY

	Fig. 4 Cases	Grasp Q_{MSV}	Grasp Q_{GII}	Grasp Q_{VEW}
Centroid Strategy	**a)**	**2.2307**	**0.9941**	**125.4403**
	h)	2.2359	0.9974	125.7573
	i)	2.2340	0.9965	125.8007
	j)	2.2260	0.9890	125.7573

Static grasp values of Q_{MSV}=2.2089, Q_{GII}=0.9749, Q_{VEW}= 125.4176.

C. *Centroid Strategy Results*

Table III shows a summary of the simulation grasp qualities for a) and h)-j). There is no significant difference between the quality of grasps across the centroid strategies. However, quantitative analysis of the grasps cannot alone inform behaviors as similar values can result from different grasps. Figure 5 shows a subset of qualitative differences between cases. Figure 5i is the static contact point cases where points will not move. Figure 5ii is the position tracking centroid strategy which resembles caging [22] by attempting to surround the cube on all faces. The middle two images are an example of equivalent grasps due to the similarity. Figure 5iv is the c_i^{VEW} grasp which attempts to move to corners and edges. Figure 5iv is a result of finger reassignment constraints since we are aware non-unique grasps could exist resulting in fingers crossing. Figure 5iii shows the damaged case of relieving 2 broken fingers.

Further, the centroid analysis needs to consider the effort of moving the contact points between time steps. A subset of the energy and distance in Figure 6 show how the weighting schemes can cause more active or less active centroid movement. From most active to least active the approaches rank as follows: c_i^{GII}, c_i^{MSV}, c_i^{VEW}, and lastly with the position tracking. Although Table III and Figure 4 (the bottom row) show they garner similar quality of grasps, the activity of each

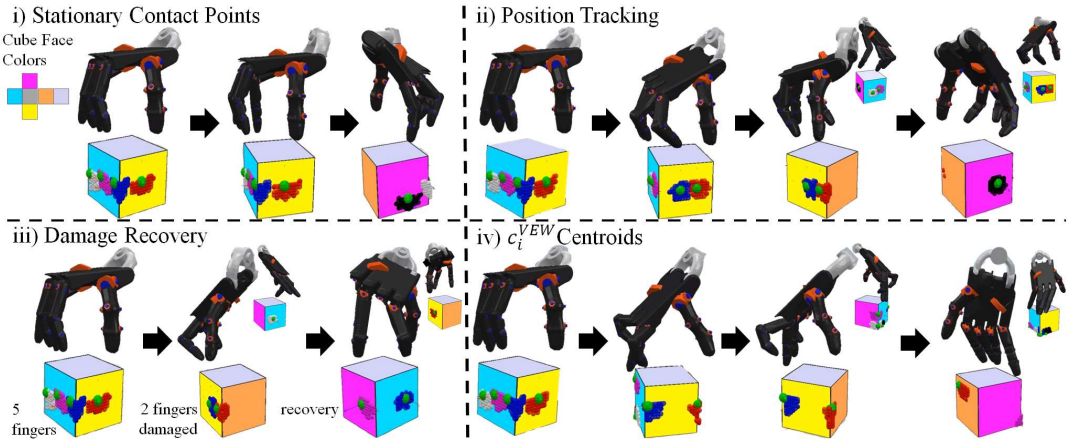

Figure 5: Centroid determination examples, the configurations are not synchronized to better show the safe regions (color clusters on the cub surfaces). i) the static contact points in green (baseline method. All other three cases started with the same initial condition as i). ii) the position tracking method and iii) is the same method for the contact points switching from 5 to 3. iv) is the centroid method using Q_{VEW} as the weighting scheme. In ii) the safe regions attempt to surround the object on the faces where the hand configuration is a smooth natural transition to all faces. The safe regions of iv) expand to the edges and corners. Since kinematic metrics currently are not being used as primary constraints, the grasps appear to be less comfortable and natural.

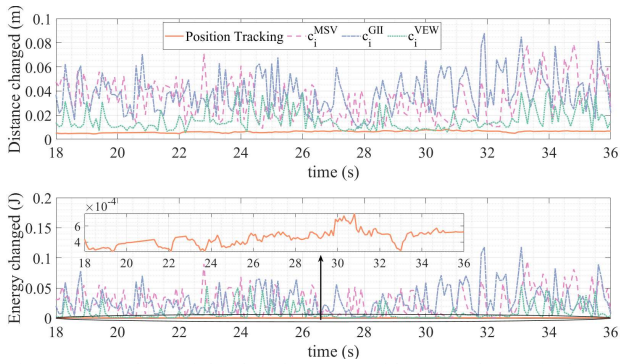

Figure 6: A subset of the data for 4 centroid cases. The top is the net distance changed between each time point for all contact points. The position tracking strategy (orange line) is stable, and lower than the other strategies. The c_i^{VEW} (green line) is lower than the other two metrics. The c_i^{MSV} (pink line) is lower than the c_i^{GII} (blue line). The same trends hold for the net energy changed (bottom row).

strategy to achieve the similar results are intriguing. For instance, a succession of multiple active points likely indicates transitional contact points to find a suitable stable configuration (searching the Y space). While small gradual changes reflect readjustment to an already stable configuration (refinement at local minimum). The difference between highly active and subtle movement does not necessarily correspond to minimizing the pre-shaping hand motion. Yet, the significance in motion demonstrates the necessity for desired behavior when hand kinematics are considered in the contact points.

V. Conclusion And Discussion

A. The Position Tracking Centroid Approach

One of the more unexpected and pleasantly surprising results from this work is seeing the position tracking method surround the cube on all faces mimicking caging schemes. This is promising as it places fingers in an intuitive way, while holding up in terms of grasp quality (Q_{MSV} = 2.2307, Q_{GII} = 0.9941, Q_{VEW} = 125.4403). The position tracking method is also the fastest centroid to compute because the other approaches compute partial grasp matrices in the safe region. The position centroid is the least active (energy and displacement) compared to the other centroid methods. Overall, it appears the most promising centroid approach.

B. Coupling Motion, Limiters, and Other Constraints

The coupling motion between c_i can occur by constraints that limit the centroid motion. This is practical if c_i correspond to kinematic chains such as the fingertip and distal joint. Coupling the motion would result in two possible outcomes: 1) a coupled pair would find the best approach for the couple, but not necessarily the best for either c_i, or 2) find the best for a single c_i and a suboptimal solution for the second.

An additional type of limitations put on the centroids is the amount of motion they are allowed. For each iteration, the centroid could update discretely and discontinuously. To provide more natural transitions, centroids could have constraints such as maximum distance/velocity allowed. Another consideration is the choice of weighting schemes. The strategies presented in this paper were independent metrics; linear combinations of them are possible [32][33][34] where this could present behavior taking advantage of all grasp metrics and positional tracking. Likewise, other metrics such as independent contact regions [35] could be used or integrated to weight the safe regions.

Certain surfaces on the objects can be considered obstacles (i.e. the cube's bottom face in contact with a table). This can be extended to ensure certain faces or parts of an object are off limits to facilitate a task need. The obstacles can act dynamically (as shown in Figure 5 as the cube moves) and the safe regions' movements still adapt to their environment. The flexibility of the safe regions allows integration of these constraints to perform a users' specifications.

C. Limitations and Considerations of the Approach

Considerations of using the multi-agent perspective to adapt contact points rely on three necessary components: 1) pose estimation of the object, and consequently, 2) defining free space (set Y) and closed space (set Z) on the objects, and 3) choosing the weighting and modeling scheme of the contact points. Although pose estimation was done by a Kalman filter with measurement data from simulation, this measurement can be achieved by other means of computer vision [28], or inertial measurement unit [36], as well as filtered by other techniques such as Partially Observable Markov Decision Process [37], or adaptive filtering [38]. Since the approach is an object-centric perspective, it requires estimation of the object pose. Defining the available points on an object requires understanding object properties (materials and shape convexity) and task constraints (where grasping is available). Defining both sets, Y and Z, is necessary which requires extensive knowledge of the robot's environment. The weighting scheme to build safe regions we proposed are based on physical limitations of the robotic hand, however, these could be based on other practical aspects such as friction and forces. Likewise, modeling the contact points as hard-finger, soft finger, point without friction [3] are alternatives which influence the safe region and centroid point.

Finger assignment and hand kinematics are not our primary focus in this paper. Explicit hand-centric grasp metrics need to be considered. Future avenues are analyzing the candidate grasps during or after the safe region development through common hand-centric grasp metrics such as the distance to singular configuration, volume of the manipulability ellipsoid, and uniformity of transformation [35].

D. Equivalent vs Non-unique Grasps

Another aspect of considering dynamic contact point adaption is determining contact points that can be solved by nonunique or equivalent grasps to achieve a task [11]. The example illustrated in [11] shows how separate finger combinations can play the same notes on a guitar. Equivalent finger configurations are those that have different positions, but the same functional purpose (i.e., overall goal and task success). With the guitar example, this is two separate configurations playing the same note. In a grasping context, this would often be observed where hand postures would look identical, but at a different location on an object to solve the same task. A non-unique solution is achieved when finger assignment for the same location is interchangeable, such as using your index finger or middle finger to play a note. In a grasping context, this would be seen in a two-finger pinching grasp where the index finger and middle finger are interchangeable. Being

cognizant of these two potential solution types is imperative when designing kinematic and c_i motion constraints.

ACKNOWLEDGEMENT

This material is based on work supported by the US NSF under grant 1652454. Any opinions, findings, and conclusions or recommendations expressed in this material are those of the authors and do not necessarily reflect those of the National Science Foundation. We would like to thank Yunsik Jung for setting up the V-REP environment.

REFERENCES

[1] T. Supuk, T. Kodek, and T. Bajd, “Estimation of hand preshaping during human grasping,” Medical Engineering and Physics, vol. 27,pp. 790–797, 11 2005.

[2] Zhengtao Zhang, De Xu and Junzhi Yu, "Research and latest development of Ping-Pong robot player," *2008 7th World Congress on Intelligent Control and Automation*, Chongqing, China, 2008, pp. 4881-4886, doi: 10.1109/WCICA.2008.4593715.

[3] D. Prattichizzo and J. C. Trinkle, “Grasping,” pp. 955–988, 2016.

[4] J.-H. Bae, S. Arimoto, Y. Yamamoto, H. Hashiguchi, and M. Sekimoto, “Reaching to grasp and preshaping of multi-DoFs robotic hand-arm systems using approximate configuration of objects.” IEEE, 2006, p.5774.

[5] Q. V. Le, D. Kamm, A. F. Kara, and A. Y. Ng, “Learning to grasp objects with multiple contact points,” 2010.

[6] R. Ozawa and K. Tahara, “Grasp and dexterous manipulation of multi-fingered robotic hands: a review from a control view point,” Advanced Robotics, vol. 31, pp. 1030–1050, 10 2017.

[7] D. Prattichizzo, M. Malvezzi, and A. Bicchi, “On motion and force control of grasping hands with postural synergies,” 2010.

[8] M. Santello, M. Bianchi, M. Gabiccini, E. Ricciardi, G. Salvietti,D. Prattichizzo, M. Ernst, A. Moscatelli, H. J ̈orntell, A. M. Kappers,K. Kyriakopoulos, A. Albu-Sch ̈affer, C. Castellini, and A. Bicchi,“Hand synergies: Integration of robotics and neuroscience for under-standing the control of biological and artificial hands,” pp. 1–23, 22016.

[9] D. Ortenzi, U. Scarcia, R. Meattini, G. Palli, and C. Melchiorri, “Synergy-based control of anthropomorphic robotic hands with contact force sensors,” vol. 52. Elsevier B.V., 9 2019, pp. 340–345.

[10] C. Piazza, M. G. Catalano, S. B. Godfrey, M. Rossi, G. Grioli, M. Bianchi, K. Zhao, and A. Bicchi, “The softhand pro-h: A hybrid body-controlled, electrically powered hand prosthesis for daily living and working,” IEEE Robotics and Automation Magazine, vol. 24, pp.87–101, 12 2017.

[11] G. Elkoura and K. Singh, “Handrix: Animating the human hand,” 2003.

[12] D. Prattichizzo, M. Malvezzi, M. Gabiccini, and A. Bicchi, “On the manipulability ellipsoids of underactuated robotic hands with compliance,” Robotics and Autonomous Systems, vol. 60, pp. 337–346, 3 2012.

[13] N. Daoud, J. P. Gazeau, S. Zeghloul, and M. Arsicault, “A real-time strategy for dexterous manipulation: Fingertips motion planning, force sensing and grasp stability,” Robotics and Autonomous Systems, vol. 60, pp. 377–386, 3 2012.

[14] R. L. Andersson, "Aggressive trajectory generator for a robot ping-pong player," in *IEEE Control Systems Magazine*, vol. 9, no. 2, pp. 15-21, Feb. 1989, doi: 10.1109/37.16766.

[15] R. I. Popescu, M. Raison, G. M. Popescu, D. Saussié, and S. Achiche, “Design and development of a novel type of table tennis aerial robot player with tilting propellers,” *Mechatronics*, vol. 74, p. 102483, 2021.

[16] R. Silva, F. S. Melo and M. Veloso, "Towards table tennis with a quadrotor autonomous learning robot and onboard vision," *2015 IEEE/RSJ International Conference on Intelligent Robots and Systems (IROS)*, Hamburg, Germany, 2015, pp. 649-655, doi: 10.1109/IROS.2015.7353441.

[17] Su K., Shen S. (2017) Catching a Flying Ball with a Vision-Based Quadrotor. In: Kulić D., Nakamura Y., Khatib O., Venture G. (eds) 2016 International Symposium on Experimental Robotics. ISER 2016. Springer Proceedings in Advanced Robotics, vol 1. Springer, Cham. https://doi.org/10.1007/978-3-319-50115-4_48

[18] R. Ritz, M. W. Müller, M. Hehn and R. D'Andrea, "Cooperative quadrocopter ball throwing and catching," *2012 IEEE/RSJ International Conference on Intelligent Robots and Systems*, Vilamoura-Algarve, Portugal, 2012, pp. 4972-4978, doi: 10.1109/IROS.2012.6385963.

[19] Marturi, N., Kopicki, M., Rastegarpanah, A. et al. “Dynamic grasp and trajectory planning for moving objects.” Auton Robot 43, 1241–1256 2019. https://doi.org/10.1007/s10514-018-9799-1

[20] J. Aleotti and S. Caselli, "Grasp recognition in virtual reality for robot pregrasp planning by demonstration," *Proceedings 2006 IEEE International Conference on Robotics and Automation, 2006. ICRA 2006.*, 2006, pp. 2801-2806, doi: 10.1109/ROBOT.2006.1642125.

[21] M. Gabiccini, A. Bicchi, D. Prattichizzo, and M. Malvezzi, “On the role of hand synergies in the optimal choice of grasping forces,” Autonomous Robots, vol. 31, pp. 235–252, 10 2011.

[22] D. Kim, Y. Maeda, and S. Komiyama, “Caging-based grasping of deformable objects for geometry-based robotic manipulation,” ROBOMECH Journal, vol. 6, 12 2019.

[23] S. Brahmbhatt, C. Ham, C. C. Kemp, and J. Hays, “Contactdb:Analyzing and predicting grasp contact via thermal imaging,” in Proceedings of the IEEE/CVF Conference on Computer Vision andPattern Recognition, 2019, pp. 8709–8719.

[24] B. Le ́on, J. L. Sancho-Bru, N. J. Jarque-Bou, A. Morales, and M. A.Roa, “Evaluation of human prehension using grasp quality measures,” International Journal of Advanced Robotic Systems, 2012.

[25] A. Pierson and D. Rus, “Distributed target tracking in cluttered environments with guaranteed collision avoidance.” IEEE, 2017.

[26] A. Pierson, L. C. Figueiredo, L. C. A. Pimenta, and M. Schwager, “Adapting to performance variations in multi-robot coverage,” 2015.

[27] J. Cort ́es, S. Mart ınez, T. Karatas, and F. Bullo, “Coverage control for mobile sensing networks,” IEEE Transactions on Robotics and Automation, vol. 20, pp. 243 –255, 2004.

[28] Du, G., Wang, K., Lian, S. *et al.* “Vision-based robotic grasping from object localization, object pose estimation to grasp estimation for parallel grippers: a review.” *Artif Intell Rev* **54,** 1677–1734 (2021). https://doi.org/10.1007/s10462-020-09888-5

[29] Doosti, S. Naha, M. Mirbagheri, and D. Crandall, “Hope-net: Agraph-based model for hand-object pose estimation,” inThe IEEEConference on Computer Vision and Pattern Recognition (CVPR), June2020.

[30] E. Rohmer, S. P. N. Signgh, and M. Freese, “V-rep: a versatile and scalable robot simulation framework.” IEEE, 2013.

[31] M. Schwager, D. Rus, and J. J. Slotine, “Decentralized, adaptive coverage control for networked robots,” International Journal of Robotics Research, vol. 28, pp. 357–375, 3 2009.

[32] J. Aleotti and S. Caselli, “Interactive teaching of task-oriented robot grasps,” Robotics and Autonomous Systems, vol. 58, pp. 539–550, 52010.

[33] E. Chinellato, R. B. Fisher, A. Morales ́angel, M. Morales ́angel, and P. D. Pobil, “Ranking planar grasp configurations for a three-finger hand,” 2003.

[34] B. H. Kim, B. J. Yi, S. R. Oh, and I. H. Suh, “Non-dimensionalized performance indices based optimal grasping for multi-fingered hands,” Mechatronics, vol. 14, pp. 255–280, 4 2004.

[35] M. A. Roa and R. Su arez, “Grasp quality measures: review and performance,” Autonomous Robots, vol. 38, pp. 65–88, 2014.

[36] M. Theiss, P. M. Scholl, and K. V. Laerhoven, “Predicting grasps with a wearable inertial and EMG sensing unit for low-power detection of in-hand objects,” vol. 25-27-February-2016. Association for Computing Machinery, 2 2016.

[37] G. Lu, W. Ouyang, D. Xu, X. Zhang, Z. Gao, and M.-T. Sun, “Deepkalman filtering network for video compression artifact reduction,” in Proceedings of the European Conference on Computer Vision (ECCV),2018, pp. 568–584.

[38] J. N. Kutz, X. Fu, S. L. Brunton, and N. B. Erichson, “Multi-resolution dynamic mode decomposition for foreground/background separation and object tracking,” vol. 2015-February.Institute of Electrical and Electronics Engineers Inc., 2 2015, pp. 921–929